

Q_P Structure of Sediments in the Kanto Plain

Kazuki KOHKETSU and Etsuzo SHIMA

Earthquake Research Institute, University of Tokyo

(Received September 28, 1985)

Abstract

The Q_P structure was derived for the sediments and the uppermost crust in the Kanto plain. Synthetic explosion seismograms were computed for causally attenuative crustal models with the elastic wave velocities determined by refraction experiments, and they were compared with observed seismograms. After some forward and inverse modelings we obtained an optimal Q_P structure, in which sedimentary layers have very low Q_P -values of 35 and 100, as against 400 for the uppermost crust.

1. Introduction

To analyze seismic source process in detail or to predict strong motions precisely, we should compute synthetic near-field seismograms for a realistic medium. Tokyo is located in the Kanto plain having thick sedimentary layers, and seismograms must be affected strongly by them within the period range of 1-10 sec in which both seismologists and earthquake engineers are interested. Therefore, it is necessary to include their effects on seismograms.

For seismogram synthesis we need structures of five physical parameters, *i. e.* P - and S -wave velocities (V_P , V_S), density (ρ), and Q -values for P - and S -waves (Q_P , Q_S). The influence of Q cannot be ignored, because even in the near field seismograms are strongly distorted by such a low Q as expected for sediments (TAKEO, 1985; KOHKETSU, 1986). The velocity structures in the Kanto plain have already been revealed by the Yumenoshima refraction experiments (SHIMA *et al.*, 1976a, b, 1978a, b, 1981) and *in situ* measurements at deep boreholes (OHTA *et al.*, 1980). The ρ and Q_S structures were also derived from down-hole measurements (TAKAHASHI and HAMADA, 1975; OHTA *et al.*, 1980; YAMAMIZU *et al.*, 1983), but we have no information about the Q_P structure.

Investigations of P -wave attenuation have been limited to surface sediments (*e. g.* AOKI, 1960; KUDO, 1973), though we have a very good P -wave generator, namely "explosion". The reason for this is supposed to be that Q_P is not essential to rough estimations of strong motions. In contrast it is indispensable for detailed estimations.

Q -value is usually obtained by comparing spectral amplitudes of seismic waves for different frequencies or those for different observation points. However, these spectral ratio methods are sometimes unstable, because they deeply depend on Fourier analysis and filtering techniques. Thus, in this study we will estimate the Q_P structure of sediments in the Kanto plain by means of comparing synthetic explosion seismograms with the records obtained from the first Yumenoshima refraction experiment (SHIMA *et al.*, 1976a) in time domain. Synthetic seismograms will be calculated using the extended reflectivity method (KIND, 1978; KOHKETSU, 1985).

2. Forward Modeling

In February, 1975, the first Yumenoshima refraction experiment was carried out to investigate the underground structure beneath the Tokyo Metropolitan Area down to the uppermost part of the Earth's crust. An explosion of 495 kg of dynamite was set off in Yumenoshima, the southmost part of the reclaimed land of Tokyo. There were 14 observation points, which are shown in Fig. 1 along with the shot point.

In the obtained record section shown in Fig. 2, a clear initial phase and a well-developed later phase can be found with apparent velocities of 5.5 and 1.8 km/sec, respectively. SHIMA *et al.* (1976a) identified them as a refraction through the uppermost crust (P_3) and a direct wave (P_0) or a reflection (PP_1) in a surface layer, and derived the three-layer (two layers and a halfspace) velocity structure given in Table 1. Travel times of P_3 , P_0 and PP_1 are indicated by thin solid lines in Fig. 2. This model excellently agrees with the results of *in situ* downhole measurements (OHTA *et al.*, 1980; YAMAMIZU *et al.*, 1981) except the halfspace corresponding to the uppermost crust. Since the halfspace derived from the downhole measurements is assumed to be a thin layer over the uppermost crust (YAMAMIZU *et al.*, 1981), we will neglect it in this study.

Densities of the three layers are estimated to be 2.0, 2.3 and 2.5 g/cm³ respectively from the downhole density profiles observed in borings by TAKAHASHI and HAMADA (1975), OHTA *et al.* (1980), and YAMAMIZU *et al.* (1981). The structure of these physical parameters, V_P , V_S and ρ is summarized in Table 1.



Fig. 1. Shot and observation points of the first Yumenoshima refraction experiment (1975). The shot point is indicated by a cross close to the lower boundary (after SHIMA *et al.*, 1976a).

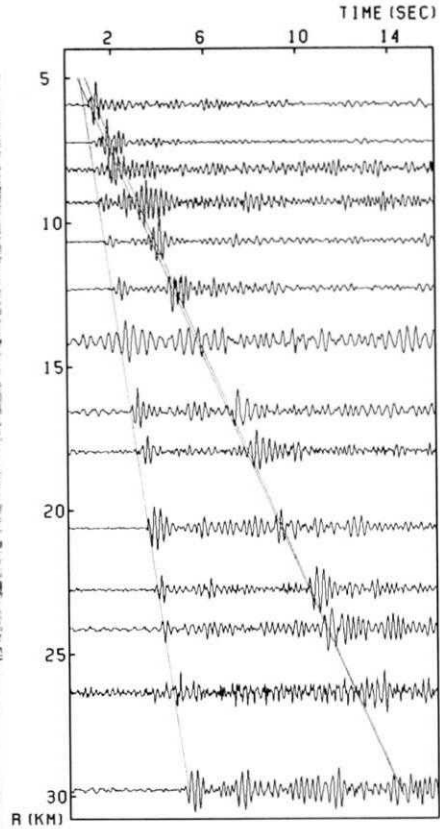


Fig. 2. Observed record section of the first Yumenoshima refraction experiment. Thin solid lines indicate travel times of P_3 , P_0 and PP_1 .

Table 1. Velocity Model.

No.	Thickness (km)	V_p (km/s)	V_s (km/s)	ρ (g/cm ³)
1	1.3	1.8	0.68	2.0
2	1.0	2.7	1.5	2.3
3		5.5	3.0	2.5

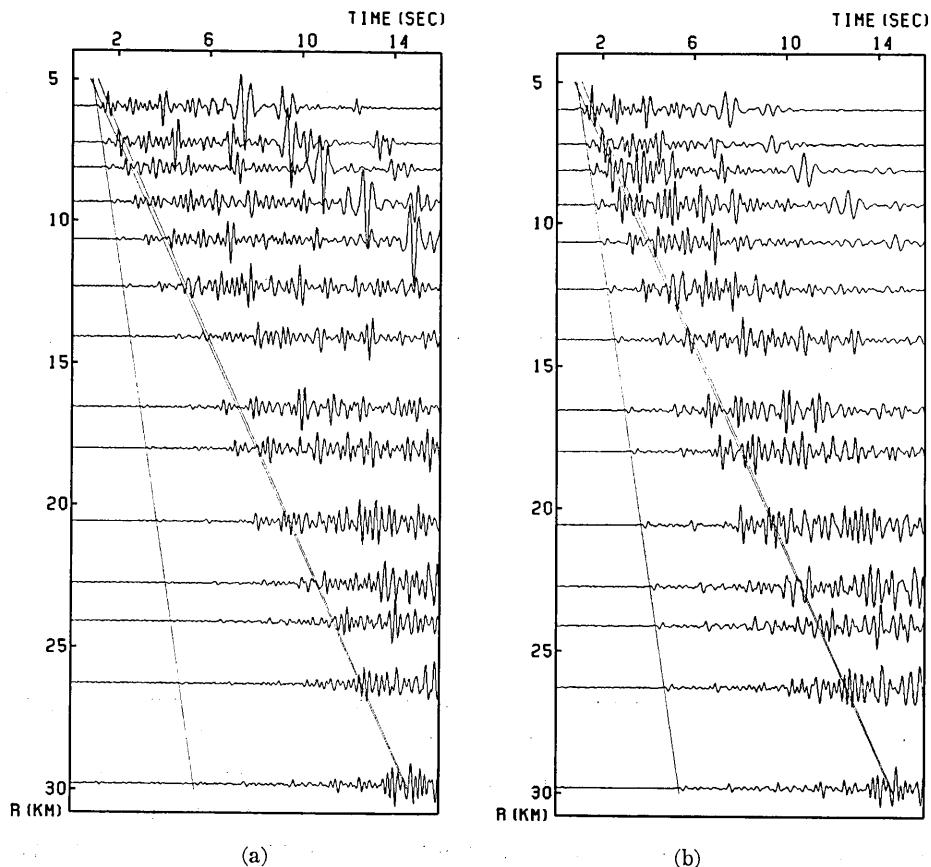
Of the two sedimentary layers the top is expected to dominate characteristics of seismograms, because it must have a very low Q_p according to its velocities and Q_s , and because the explosive source was situated in it. Therefore we computed seismograms for the crustal model of Table 1 with various Q_p -values of the top layer. The second layer and the half-

space remain perfectly elastic in this section. To compute synthetic seismograms for attenuative layered media we used the extended reflectivity method (KIND, 1978; KOHKETSU, 1985), which can generate complete seismograms implicitly including surface waves and all multiple reflections.

From the possibility of low Q -values for the sedimentary layers, we introduced causal absorption presented by several authors (*e. g.* FUTTERMAN, 1962; KANAMORI and ANDERSON, 1977). Many observations show constant Q at frequencies below 1 Hz. In addition KUDO and SHIMA (1970) observed it at frequencies over 10 Hz. Then phase velocities were made complex with frequency-independent Q as

$$c = c_r \left[1 + \frac{1}{\pi Q} \log \left(\frac{f}{f_r} \right) + \frac{i}{2Q} \right], \quad (1)$$

following O'NEIL and HILL (1979). To use the velocities in Table 1 as reference velocities c_r we specified the reference frequency f_r to be the



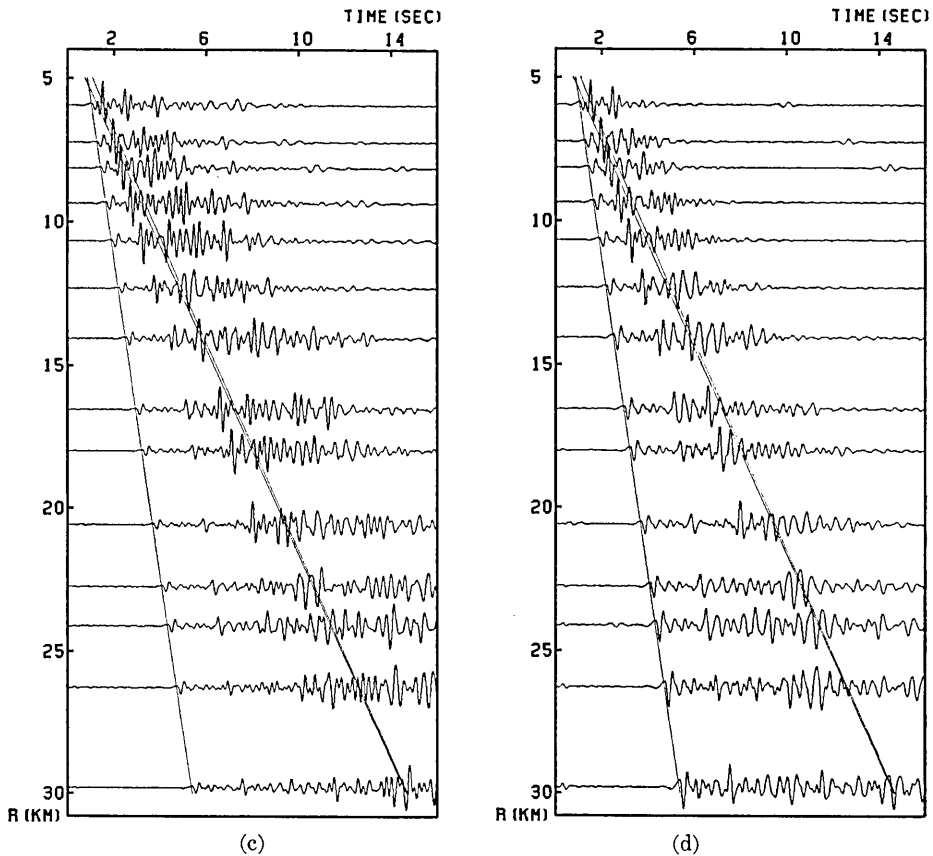


Fig. 3. Synthetic record sections computed with the Q_P of the surface layer equal to (a) ∞ , (b) 100, (c) 50 and (d) 20.

predominant frequency of signals, *i. e.* 5 Hz.

Figure 3 shows four synthetic record sections which were computed with Q_P -values of the top layer equal to (a) ∞ , (b) 100, (c) 50, (d) 20. Since Q_S hardly affects explosion seismograms, it was derived by the approximated relation $Q_S/Q_P=4/9$. As a source time function we used the smoothed ramp function of HERRMANN (1979) with a rise time of 0.3 sec. Each trace in the sections is normalized to its maximum amplitude. Thin solid lines indicate the travel times of P_3 , P_0 and PP_1 as in the observed record section. Since well-developed Rayleigh waves suppress earlier phases, five traces at distances shorter than 12 km were amplified by a factor of two in Fig. 3(a).

All the sections do not well simulate P_0 and PP_1 , because they are contaminated by multiple reflections whose apparent velocity is equal to that of P_3 . In the observed section of Fig. 2 the first-order multiple can

be seen about two seconds after P_3 , but the second- and higher-order multiples are not found with such large amplitudes as seen in the synthetic record sections. However, from comparing them we can make the following points.

- (1) In the sections for $Q_P = \infty$ and 100, reverberation phases and surface waves coming after P_0 and PP_1 dominate the seismograms.
- (2) The situation is better in sections (c) and (d) for $Q_P = 50$ and 20. However, the amplitude of P_3 is still small in (c). On the other hand, in (d) we can find no significant phases on and after the travel time of P_0 or PP_1 .

From the above two points the Q_P -value of the top layer is expected to be between 50 and 20. We will not advance our forward modeling from this rough estimation, because the Q -values of the lower part of the model and the source time function affect synthetic seismograms and we should take them into consideration. Instead, a kind of inverse modeling should be introduced to determine these many parameters meaningfully.

3. Inverse Modeling

A simple and fast method of seismogram synthesis is necessary for inverse modeling. ČERVENÝ and FRANGIÉ (1980, 1982) derived an explicit expression for the waveform of the Gavor wavelet deformed by an attenuative medium. After the Gavor wavelet

$$u(t) = \exp(-2\pi f_0 t / \gamma)^2 \cos(2\pi f_0 t + \nu) \quad (2)$$

propagates through a causally attenuative medium whose velocity is specified by Eq. (1), its deformed waveform is expressed by

$$u(x, t) = \exp[-(2\pi f_0 T / \gamma)^2 - (\pi f_0 t^* / \gamma)^2 - \pi f^* t^*] \\ \times \cos[2\pi f^*(T - \pi^{-1} t^*) + \nu] \quad (3)$$

with

$$T = t - x/c(f_0) + (t^*/\pi)[1 + \log(f^*/f_0)] \\ f^* = f_0(1 - 2\pi f_0 t^* / \gamma^2). \quad (4)$$

We use the predominant frequency f_0 of the wavelet as a reference frequency f_r in Eq. (1). γ and ν express envelope shape and phase shift of the wavelet. t^* is a global absorption factor summed up along the propagation path x , that is,

$$t^* = \int \frac{dx}{c_r Q}. \quad (5)$$

When the stratification effect of media is evaluated by the ray theory of ČERVENÝ and RAVINDRA (1971), we can easily compute synthetic seismograms for specified phases.

In order to determine uniquely the *Q*-values of the three layers, an iterative waveform inversion was applied by means of minimizing the difference of data and ray-theoretical waveforms for *P*₃ and *PP*₁. *P*₀ was neglected, because after some ray-theoretical calculations we found that *PP*₁ has a much greater amplitude than *P*₀ for the crustal model of Table 1. Among the observed seismograms beyond 10 km where *P*₃ and *PP*₁ are clearly separated, the four traces at distances from 13 km to 21 km have larger *P*₃ than others. Since this must be due to local site effects, we adopted the *P*₃ and *PP*₁ portions at 10.66, 22.75 and 24.11 km as data seismograms. The traces at 12.31, 26.27 and 29.80 km were omitted because of instrumental saturation or low signal-to-noise ratio.

We concentrate our attention to waveforms and relative amplitudes of *P*₃ and *PP*₁, because fluctuations of travel time and unreliable absolute amplitudes may break down the inversion. To remove errors in travel time and absolute amplitude, we evaluated the difference between data and synthetic seismograms with the error function

$$d_i = \frac{\int (f_i(t) - s_i(t - t^*)) dt}{\left[\int f_i^2(t) dt \right]^{1/2} \left[\int s_i^2(t - t^*) dt \right]^{1/2}}, \quad (6)$$

where *f_i* is the *i*-th data seismograms, *s_i* is the *i*-th synthetic seismograms and *t** is the time shift which minimizes the deviation of *s_i* from *f_i*. *d_i* is derived from the error function of MELLMAN (1980) by replacing a cross-correlation function with a simple deviation.

The parameters *f*₀, *γ* and *ν* specifying the source wavelet were taken as independent variables in addition to the *Q_P*-values. A least-squares inversion was performed in a Gauss-Newton style neglecting second- and higher-order derivatives of the error functions. The three layers were given 50, 100 and 500 as initial values of *Q_P* (Table 2). Those of *f*₀, *γ* and *ν* were 4, 7 and 3π/2, which were selected by advance fittings. To stabilize the inversion we introduced "weak" equality constraints (LAWSON and

Table 2. Starting and Resultant Models.

<i>Q_{P1}</i>	<i>Q_{P2}</i>	<i>Q_{P3}</i>	<i>f</i> ₀	<i>γ</i>	<i>ν</i>
50	100	500	4.0	7.0	270°
37.2	99.5	406	3.97	7.14	272°

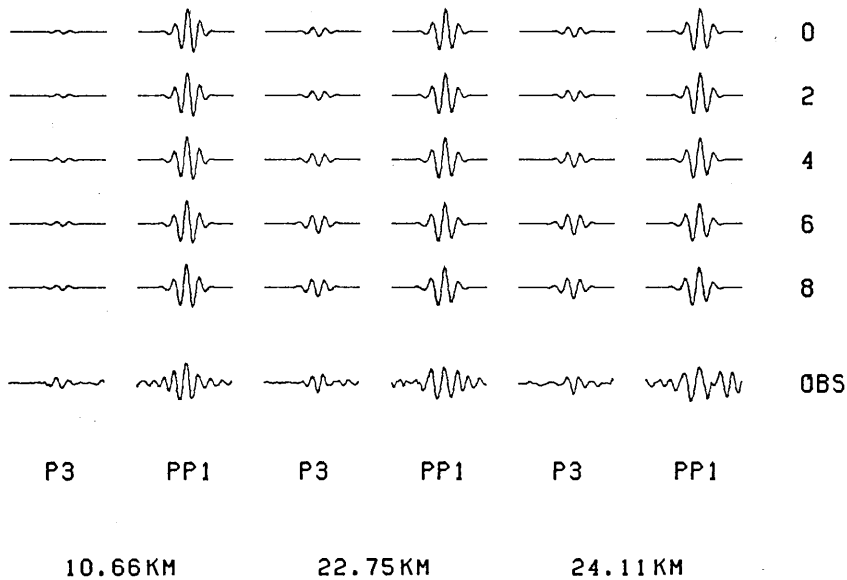


Fig. 4. The progression of ray-theoretical waveforms from the starting model through eight iterations. The observed waveforms are shown at the bottom with letters OBS.

HANSON, 1974; NAKAGAWA and KOYANAGI, 1982) in which the variables are required to be close to the initial values within standard deviations ten times larger than the initial values. Only the Q_P of the top layer was constrained twice more tightly than others, because we have already estimated that it falls between 50 and 20.

Figure 4 illustrates the progression of waveforms as the inversion proceeded. After eight iterations we obtained the final model shown in Table 2. Such a good fit to the observed seismograms as the final model had been obtained at the sixth stage of iteration. The top layer is given a very low Q_P , 37.2. It is due to the good advance fittings that the final values of the source wavelet parameters are very close to the initial values.

At this stage we should note that we ignored interference by phases other than P_3 and PP_1 . The ray theory itself is not so accurate for the considered frequency range and space dimensions (ČERVENÝ *et al.*, 1977). Thus we confirm the inversion result with reflectivity seismograms.

The synthetic record section shown in Fig. 5 was computed by the extended reflectivity method with the final parameter values. The Q_P -values were rounded as in Table 3. Following YAMAMIZU *et al.* (1983), we adopted $Q_s=20$, 50 and 200 for the three layers from top to bottom. They analyzed S -waves from a SH -wave generator observed in a 2,300

Table 3. Velocity and Attenuation Model.

No.	Thickness (km)	V_p (km/s)	V_s (km/s)	ρ (g/cm ³)	Q_P	Q_S
1	1.3	1.8	0.68	2.0	35	20
2	1.0	2.7	1.5	2.3	100	50
3		5.5	3.0	2.5	400	200

meter-borehole using the spectral ratio method. Since the borehole does not reach the 5.5 km/sec part of the crust, the Q_s of the halfspace is a little higher than their original value, 155. The Gavor wavelet was used as an input signal with the obtained parameters.

The agreement to the observed record section is improved in Fig. 5. However, beyond 20 km we again find higher-order multiple reflections with apparent velocities 5.5 km/sec and large amplitudes as seen in Fig. 3. To remove this discrepancy we should modify the velocity structure, especially the velocity of the second layer which was not determined so exactly by SHIMA *et al.* (1976a).

4. Conclusion

The Q_P structure was derived for the sediments and the uppermost crust in the Kanto plain by means of comparing observed explosion seismograms with synthetics for causally attenuative media. $Q_P=35, 100$ and 400 were obtained for the three velocity layers inferred from the Yumenoshima refraction experiments.

The synthetic record section for the final Q_P model successfully simulates the observed section, but multiple reflections with apparent velocities of 5.5 km/sec are more distinctly developed than observed. We should modify the velocity structure to remove this defect.

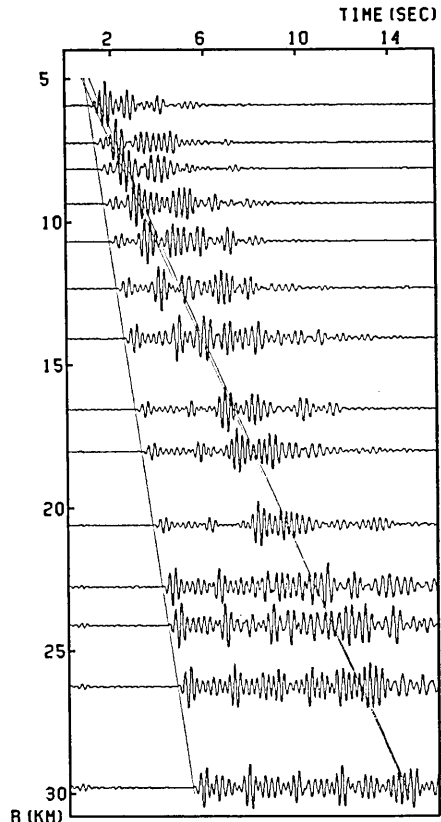


Fig. 5. Synthetic record section computed with the obtained Q_P -values and the Q_S -values by YAMAMIZU *et al.* (1983).

Acknowledgement

We would like to thank members of the Shutoken Kiban Kozo Kenkyu Group for their work during the experiments. We are also grateful to Dr. Červený for communication about his works. Miss M. Harasawa kindly performed *A/D* conversions and instrumental corrections for recorded seismograms.

This study was supported by Grants-in-Aid for Scientific Research No. 57025011 and 59025009 from the Ministry of Education, Science and Culture of Japan.

References

- AOKI, H., 1960, Seismic waves in the region near explosive origin, *J. Earth Sci. Nagoya Univ.*, 8, 120-173.
- ČERVENÝ, V. and A. B. FRANGIÉ, 1980, Elementary seismograms of seismic body waves in dissipative media, *Studia Geophys. Geod.*, 24, 365-372.
- ČERVENÝ, V. and A. B. FRANGIÉ, 1982, Effects of causal absorption on seismic body waves, *Studia Geophys. Geod.*, 26, 238-253.
- ČERVENÝ, V., I. A. MOLOTKOV and I. PŠENČIK, 1977, *Ray Method in Seismology*, Univerzita Karlova, Praha.
- ČERVENÝ, V. and R. RAVINDRA, 1971, *Theory of Seismic Head Waves*, Univ. Toronto Press, Toronto.
- FUTTERMAN, W. I., 1962, Dispersive body waves, *J. Geophys. Res.*, 67, 5279-5291.
- HERRMANN, R. B., 1979, SH-wave generation by dislocation sources. A numerical study, *Bull. Seismol. Soc. Am.*, 69, 1-15.
- KANAMORI, H. and D. L. ANDERSON, 1977, Importance of physical dispersion in surface wave and free oscillation problems, Review, *Rev. Geophys. Space Phys.*, 15, 105-112.
- KIND, R., 1978, The reflectivity method for a buried source, *J. Geophys.*, 44, 603-612.
- KOHKETSU, K., 1985, The extended reflectivity method for synthetic near-field seismograms, *J. Phys. Earth*, 33, 121-131.
- KOHKETSU, K., 1986, Importance of sedimentary layers in interpreting near-field seismograms (in preparation).
- KUDO, K., 1973, Jinko-Hasaitai wo Tuka suru Hagun ni tuite, *Contributions to the Seismic Exploration Group of Japan*, 64, 1-10 (in Japanese).
- KUDO, K. and E. SHIMA, 1970, Attenuation of shear waves in soil, *Bull. Earthq. Res. Inst., Univ. Tokyo*, 48, 145-158.
- LAWSON, C. L. and R. J. HANSON, 1974. *Solving Least Squares Problems*, Prentice-Hall, Englewood Cliffs, New Jersey.
- MELLMAN, G. R., 1980, A method of body-wave waveform inversion for the determination of earth structure, *J. R. astr. Soc.*, 62, 481-504.
- NAKAGAWA, T. and Y. KOYANAGI, 1982. *Saisho-Jijoho ni yoru Jikken Data Kaiseki*, Univ. Tokyo Press, Tokyo (in Japanese).
- OHTA, Y., N. GOTO, F. YAMAMIZU and H. TAKAHASHI, 1980, S-wave velocity measurements in deep soil deposit and bedrock by means of an elaborated down-hole method, *Bull. Seismol. Soc. Am.*, 70, 363-377.
- O'NEIL, M. E. and D. P. HILL, 1979, Causal absorption: Its effect on synthetic seismograms computed by the reflectivity method, *Bull. Seismol. Soc. Am.*, 69, 17-25.

- SHIMA, E., M. YANAGISAWA, K. KUDO, T. YOSHII, Y. ICHINOSE, K. SEO, K. YAMAZAKI, N. OHBO, Y. YAMAMOTO, Y. OGUCHI and M. NAGANO, 1976a, On the base rock of Tokyo, *Bull. Earthq. Res. Inst., Univ. Tokyo*, 51, 1-11 (in Japanese).
- SHIMA, E., M. YANAGISAWA, K. KUDO, K. SEO and K. YAMAZAKI, 1976b, On the base rock of Tokyo. II, *Bull. Earthq. Res. Inst., Univ. Tokyo*, 51, 45-61 (in Japanese).
- SHIMA, E., M. YANAGISAWA, K. KUDO, T. YOSHII, K. SEO and K. KUROHA, 1978a, On the base rock of Tokyo. III, *Bull. Earthq. Res. Inst., Univ. Tokyo*, 53, 305-318 (in Japanese).
- SHIMA, E., M. YANAGISAWA, K. KUDO, T. YOSHII, K. SEO, N. OHBO, T. HOSHINO and M. NAGANO, 1978b, On the base rock of Tokyo. IV, *Bull. Earthq. Res. Inst., Univ. Tokyo*, 53, 1245-1255 (in Japanese).
- SHIMA, E., M. YANAGISAWA and K. KUDO, 1981, On the base rock of Tokyo. V, *Bull. Earthq. Res. Inst., Univ. Tokyo*, 56, 265-276 (in Japanese).
- TAKAHASHI, H. and K. HAMADA, 1975, Deep-borehole observation of the Earth's crust activities around Tokyo —Introduction of the Iwatsuki observatory, *Pure Appl. Geophys.*, 113, 311-320.
- TAKEO, M., 1985, Near-field synthetic seismograms taking into account the effects of anelasticity, *Papers Meteorol. Geophys.* (submitted).
- YAMAMIZU, F., H. TAKAHASHI, N. GOTO and Y. OHTA, 1981, Shear wave velocities in deep soil deposits, Part III, *Zisin (J. Seismol. Soc. Japan)*, 34, 465-479 (in Japanese).
- YAMAMIZU, F., N. GOTO, Y. OHTA and H. TAKAHASHI, 1983, Attenuation of shear waves in deep soil deposits as revealed by down-hole measurements in the 2,300 meter-borehole of the Shimohsa observatory, Japan, *J. Phys. Earth*, 31, 139-157.

関東平野における堆積層の Q_P 構造

地震研究所 { 瀬 瀬 一 起
 { 嶋 悦 三

関東平野における堆積層、及び地殻最上部の Q_P (P 波に対する Q 値) を求めた。第1回夢の島爆破実験の走時解析から求められた速度構造を用い、因果律を満たす Q 構造を与えて理論的な爆破波形を計算して、観測された波形と比較する方法を採用した。試行錯誤的な方法と最小自乗法を組み合わせモデル化を行なった結果、速度構造の第1,2層 ($V_p=1.8, 2.7$ km/sec) の $Q_P=35, 100$ は、地殻最上部と思われる第3層 ($V_p=5.5$ km/sec) の $Q_P=400$ と比べ、非常に小さいことがわかった。